General solution of contradirectional two-wave mixing with partially coherent waves in photorefractive crystals

Xianmin Yi, Changxi Yang, and Pochi Yeh

Department of Electrical and Computer Engineering, University of California, Santa Barbara, California 93106

Shiuan-Huei Lin and Ken Yuh Hsu

Institute of Electro-Optical Engineering, National Chiao Tung University, 1001 Ta Hsueh Road, Hsinchu, Taiwan

Received June 13, 1996; revised manuscript received November 20, 1996

We investigate contradirectional two-wave mixing with partially coherent waves in photorefractive crystals. By use of a statistical theory on linear systems, a general formulation of the problem in the space and frequency domain is derived and implemented numerically. We obtain results on beam intensity and mutual coherence. The results on the enhancement of mutual coherence are compared with previous theoretical results on simpler cases and with experimental measurements. Excellent agreements are achieved. The results also indicate that the effective interaction length can be significantly longer than the coherence length of the waves. © 1997 Optical Society of America [S0740-3224(97)01906-1]

1. INTRODUCTION

Two-wave mixing in photorefractive crystals has been investigated extensively for many applications including image amplification, laser-beam cleanup, spatial light modulators, thresholding, and power-limiting devices.[1,2] Most of the theoretical works in this area are based on wave-mixing with mutually coherent waves.[1,2] However, in some applications, such as self-pumped and mutually pumped phase-conjugate mirrors[3–6] and photorefractive filters,[7] the effect of partial temporal coherence in a two-wave-mixing process cannot be ignored. Two-wave mixing with partially coherent waves has been studied previously for the case of transmission-grating interaction.[8] In the case of transmission-grating interaction the optical path difference between the two interacting waves remains approximately the same as the two waves propagating codirectionally through the photorefractive medium, especially when the incident angles of the two waves are close to each other.[9] In the case of reflection-grating interaction the optical path difference between the two interacting waves varies significantly as the two waves propagate contradirectionally through the photorefractive medium. Thus for the case of transmission-grating interaction, only one free variable for the position is needed to describe in a self-consistent way the second-order statistical properties of the two optical waves, i.e., their intensities and mutual coherence, while at least two free variables, one for the position and one for the optical path difference, will be needed for the case of reflection-grating interaction. Another difficulty in studying the reflection-grating interaction of partially coherent waves is to find a way to incorporate the complete boundary conditions into the theoretical formulation as a result of the two-point boundary-value problem. In such a problem a complete set of boundary conditions includes both the second-order self-statistical properties (e.g., self-coherence) of each wave at its entrance boundary and the second-order mutual statistical properties (e.g., mutual coherence) of the two waves at their respective entrance boundaries. In a recent work we provided a theoretical formulation of the problem in the space and time domain for the reflection-grating interaction in the nondepleted-pump regime.[9] By using the nondepleted-pump approximation, we reduced the two-point boundary-value problem to an initial value problem. In this paper we present a general formulation of the problem in the space and frequency domain based on the standard statistical theory on linear systems. The general formulation is also implemented numerically. Specifically, we investigate the signal-intensity gain and the mutual coherence in the contradirectional wave mixing of two partially coherent waves. Contrary to conventional belief, we discover that the effective interaction length (or grating length) can be significantly longer than the coherence length of the incident waves. The results are also compared with previous theoretical results on simpler cases and with experimental measurements.

2. THEORETICAL MODEL

Photorefractive two-wave mixing is a nonlinear optical process. Because of the mutual coherence of the two waves, a dynamic holographic grating is formed in the medium. Its position and index profile are nearly stationary under the condition of a cw illumination. Both waves are scattered into each other by the presence of this index grating. Scattering of partially coherent waves by a stationary grating can be modeled with a statistical theory on linear systems.[10] An iterative procedure can subsequently be devised to obtain the final pho-

0740-3224/97/0601396-11$10.00

torefractive grating profile from an initially arbitrary grating profile.

As is shown in Fig. 1, two counter propagating waves with partial coherence enter a photorefractive medium at $z = 0$ and $z = L$, respectively. The electric field in the photorefractive medium can be written as

$$\mathbf{E}(z, t) = \mathbf{E}_1(z, t)\exp(-i\omega_0 t + i\mathbf{k}_0 z) + \mathbf{E}_2(z, t)\exp(-i\omega_0 t - i\mathbf{k}_0 z), \quad (1)$$

where ω_0 is the center frequency of the two partially coherent waves, $\mathbf{k}_0 = n\omega_0/c$ is the corresponding wave vector, and n is the refractive index of the photorefractive medium. Reflecting the partial coherence, $\mathbf{E}_1(z, t)$ and $\mathbf{E}_2(z, t)$ are stationary random variables. They represent the random fluctuation of the amplitudes of the two waves. For the convenience of our later discussion we will now briefly describe some notations and definitions for the second-order statistical properties of the two optical waves. Let $\Gamma_{11}(z, \tau) \equiv \langle \mathbf{E}_1(z, t_1)\mathbf{E}_1^*(z, t_2)\rangle$ and $\Gamma_{22}(z, \tau) \equiv \langle \mathbf{E}_2(z, t_1)\mathbf{E}_2^*(z, t_2)\rangle$ denote the self-coherence functions of $\mathbf{E}_1(z, t_1)$ and $\mathbf{E}_1(z, t_1)$, respectively, and $\Gamma_{12}(z, \tau) \equiv \langle \mathbf{E}_1(z, t_1)\mathbf{E}_2^*(z, t_2)\rangle$ be the mutual-coherence function between $\mathbf{E}_1(z, t_1)$ and $\mathbf{E}_2(z, t_2)$, where $\tau = t_1 - t_2$ is the time delay and $\langle\ \rangle$ means ensemble average. Let $\mathbf{E}_{11}(z, \Delta\omega)$ and $\mathbf{E}_{22}(z, \Delta\omega)$ denote the self-spectral-density functions of $\mathbf{E}_1(z, t)$ and $\mathbf{E}_2(z, t)$, respectively, and $\mathbf{E}_{12}(z_1, z_2, \Delta\omega)$ be the cross-spectral-density function between $\mathbf{E}_1(z_1, t)$ and $\mathbf{E}_2(z_2, t)$. The spectral-density functions and the corresponding coherence functions are Fourier-transform pairs, i.e.,

$$\Gamma_{11}(z, \tau) = \int \mathbf{E}_{11}(z, \Delta\omega)\exp(-i\Delta\omega\tau)\mathrm{d}\Delta\omega, \quad (2)$$

$$\Gamma_{22}(z, \tau) = \int \mathbf{E}_{22}(z, \Delta\omega)\exp(-i\Delta\omega\tau)\mathrm{d}\Delta\omega, \quad (3)$$

$$\Gamma_{12}(z, \tau) = \int \mathbf{E}_{12}(z, z, \Delta\omega)\exp(-i\Delta\omega\tau)\mathrm{d}\Delta\omega, \quad (4)$$

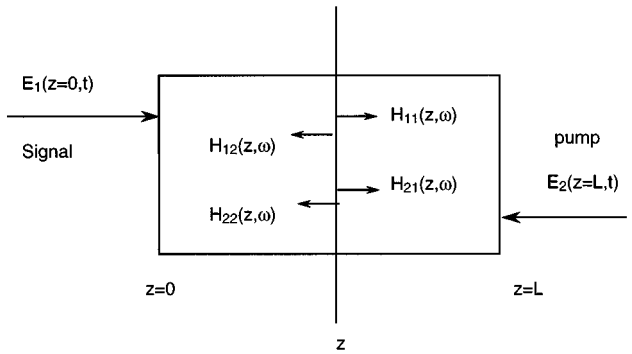

Fig. 1. Two-wave mixing in photorefractive crystals modeled as a linear system with the signal-wave entrance plane and the pump-wave entrance plane as two input planes and any arbitrary plane inbetween as the output plane.

where $\Delta\omega = \omega - \omega_0$, with ω being a general frequency component of the waves. With the above notations and relations the intensity of the two waves can be expressed as

$$I_1(z) \equiv \Gamma_{11}(z, 0) = \int \mathbf{E}_{11}(z, \Delta\omega)\mathrm{d}\Delta\omega, \quad (5)$$

$$I_2(z) \equiv \Gamma_{22}(z, 0) = \int \mathbf{E}_{22}(z, \Delta\omega)\mathrm{d}\Delta\omega, \quad (6)$$

and the mutual coherence of the two waves can be expressed as

$$\Gamma_{12}(z, 0) = \int \mathbf{E}_{12}(z, z, \Delta\omega)\mathrm{d}\Delta\omega. \quad (7)$$

With these equations the intensity of the waves as well as the mutual coherence can be obtained as soon as the spectral-density functions are obtained. In what follows we will derive the spectral-density functions by using the statistical approach.

Using the above notations and definitions, we now begin our discussion on the photorefractive interaction. Inside the photorefractive medium, a dynamic index grating is generated. It can be written as

$$\delta n = -i\frac{\gamma}{2}\frac{c}{\omega_0}\left[\frac{\mathbf{Q}(z, t)}{I_0(z)}\exp(2i\mathbf{k}_0 z) + \text{c.c.}\right], \quad (8)$$

where $\mathbf{Q}(z, t)$ is a measure of the index grating, γ is the intensity coupling coefficient, and $I_0(z) = I_1(z) + I_2(z)$ is the total intensity at position z. For the purpose of our discussion we will call $\mathbf{E}_1$ the signal wave and $\mathbf{E}_2$ the pump wave. Thus for a photorefractive grating with a positive γ, the signal wave $\mathbf{E}_1$ can be amplified. If the photorefractive effect is based purely on carrier diffusion (e.g., $BaTiO_3$,) the dynamics of the index grating is described by the following equation:

$$\tau_{\text{ph}}\frac{\partial\mathbf{Q}(z, t)}{\partial t} + \mathbf{Q}(z, t) = \mathbf{E}_1(z, t)E_2^*(z, t), \quad (9)$$

where τ_{ph} is the relaxation-time constant. By virtue of photoexcitations, photorefractive processes are usually slow at low intensities. It is reasonable to assume that the coherence time $\delta\omega^{-1}$ of the two partially coherent waves is much smaller than the relaxation time τ_{ph} of the photorefractive medium, i.e., $\delta\omega\tau_{\text{ph}} \gg 1$. Since $\mathbf{E}_1(z, t)$ and $\mathbf{E}_2(z, t)$ are stationary random variables, we can make the following approximation (see Appendix A)[8]:

$$\mathbf{Q}(z, t) \cong \langle \mathbf{Q}(z, t)\rangle = \Gamma_{12}(z, 0). \quad (10)$$

In other words, two partially coherent waves with their complex amplitudes fluctuating randomly with time can actually write a stationary grating in a photorefractive medium under the appropriate conditions. For simplicity we will denote $\mathbf{Q}(z, t)$ with $\mathbf{Q}(z)$ from now on. Note that $\mathbf{Q}(z)$ is also the mutual coherence of the two waves at position z. We note that the approximation is also valid when $\delta\omega\tau_{\text{ph}} \ll 1$.

Given arbitrary functions of $\mathbf{Q}(z)$ and $I_0(z)$, Eq. (8) yields an index grating. The propagation of a monochromatic wave through such an index grating can be described by the coupled wave equations. The coupled monochromatic waves can be written as

$$\tilde{\mathbf{E}} = \tilde{\mathbf{E}}_1(z, \omega)\exp(-i\omega t + i\mathbf{k}z) + \tilde{\mathbf{E}}_2(z, \omega)\exp(-i\omega t - i\mathbf{k}z), \quad (11)$$

where $\tilde{\mathbf{E}}_1$ and $\tilde{\mathbf{E}}_2$ are the amplitudes of the monochromatic components, ω is the optical wave frequency, and $\mathbf{k} = n\omega/c$ is the optical wave vector. The coupled wave equations can be written as

$$\frac{\partial\tilde{\mathbf{E}}_1(z, \omega)}{\partial z} = \frac{\gamma}{2I_0(z)}\mathbf{Q}(z)\tilde{\mathbf{E}}_2(z, \omega)\exp(-2i\Delta\mathbf{k}z) - \frac{\alpha}{2}\tilde{\mathbf{E}}_1(z, \omega), \quad (12)$$

$$\frac{\partial\tilde{\mathbf{E}}_2(z, \omega)}{\partial z} = \frac{\gamma}{2I_0(z)}\mathbf{Q}^*(z)\tilde{\mathbf{E}}_1(z, \omega)\exp(2i\Delta\mathbf{k}z) + \frac{\alpha}{2}\tilde{\mathbf{E}}_2(z, \omega), \quad (13)$$

where $\Delta\mathbf{k} = \mathbf{k} - \mathbf{k}_0$ is the phase mismatch between the optical waves and the index grating and α is the intensity absorption coefficient. With sufficient boundary conditions, Eqs. (12) and (13) can be solved either analytically in some special cases or numerically in general. When the boundary conditions are $\tilde{\mathbf{E}}_1(z = 0, \omega) = 1$ and $\tilde{\mathbf{E}}_2(z = L, \omega) = 0$, the solutions (output) are denoted as $\tilde{\mathbf{E}}_1(z, \omega) = \mathbf{H}_{11}(z, \omega)$ and $\tilde{\mathbf{E}}_2(z, \omega) = \mathbf{H}_{12}(z, \omega)$. When the boundary conditions are $\tilde{\mathbf{E}}_1(z = 0, \omega) = 0$ and $\tilde{\mathbf{E}}_2(z = L, \omega) = 1$, the solutions (output) are denoted as $\tilde{\mathbf{E}}_1(z, \omega) = \mathbf{H}_{21}(z, \omega)$ and $\tilde{\mathbf{E}}_2(z, \omega) = \mathbf{H}_{22}(z, \omega)$. As a linear system, the general solutions are linear combinations of $\mathbf{H}_{11}$, $\mathbf{H}_{12}$, $\mathbf{H}_{21}$, and $\mathbf{H}_{22}$.

In each of the iterations an arbitrary stationary index grating can be considered as a linear system. Referring to Fig. 1, we consider a given stationary index grating in the photorefractive medium as a linear system with the optical waves at the boundary planes $z = 0$ and $z = L$ as the input and the optical waves at an arbitrary plane z as the output. According to the theory on the statistical properties of linear systems, the second-order statistical properties of the optical waves at the output plane can be expressed in terms of the second-order statistical properties of the optical waves at the input planes and the frequency response of the linear system. To be specific, the input at the $z = 0$ plane is $\mathbf{E}_1(z = 0, t)$, the input at $z = L$ plane is $\mathbf{E}_2(z = L, t)$, and the outputs at the z plane are $\mathbf{E}_1(z, t)$ and $\mathbf{E}_2(z, t)$. The frequency response of this linear system can be expressed in terms of the solutions of Eqs. (12) and (13). With the notations described in the previous paragraph, the frequency responses from the input $\mathbf{E}_1(z = 0, t)$ to the outputs $\mathbf{E}_1(z, t)$ and $\mathbf{E}_2(z, t)$ are

$$\mathbf{H}_{11}'(z, \omega) = \mathbf{H}_{11}(z, \omega)\exp(i\Delta\mathbf{k}z), \quad (14)$$

$$\mathbf{H}_{12}'(z, \omega) = \mathbf{H}_{12}(z, \omega)\exp(-i\Delta\mathbf{k}z), \quad (15)$$

respectively. Similarly, the frequency responses from the input $\mathbf{E}_2(z = L, t)$ to the outputs $\mathbf{E}_1(z, t)$ and $\mathbf{E}_2(z, t)$ are

$$\mathbf{H}_{21}'(z, \omega) = \mathbf{H}_{21}(z, \omega)\exp(i\Delta\mathbf{k}L)\exp(i\Delta\mathbf{k}z), \quad (16)$$

$$\mathbf{H}_{22}'(z, \omega) = \mathbf{H}_{22}(z, \omega)\exp(i\Delta\mathbf{k}L)\exp(-i\Delta\mathbf{k}z), \quad (17)$$

respectively. The additional phase terms in Eqs. (14)–(17) account for the difference $\Delta\mathbf{k} = \mathbf{k} - \mathbf{k}_0$ owing to a finite $\Delta\omega = \omega - \omega_0$. With these spectral-response functions we can express the spectral-density functions of the two outputs $\mathbf{E}_1(z, t)$ and $\mathbf{E}_2(z, t)$ in terms of the spectral-density functions of the two inputs $\mathbf{E}_1(z = 0, t)$ and $\mathbf{E}_2(z = L, t)$. Thus, according to their definitions and Eqs. (14)–(17), we obtain

$$\begin{aligned}\mathbf{E}_{11}(z, \Delta\omega) = {} & \mathbf{H}_{11}(z, \omega)\mathbf{H}_{11}^*(z, \omega)\mathbf{E}_{11}(z = 0, \Delta\omega) \\ & + \mathbf{H}_{21}(z, \omega)\mathbf{H}_{21}^*(z, \omega)\mathbf{E}_{22}(z = L, \Delta\omega) \\ & + \mathbf{H}_{11}(z, \omega)\mathbf{H}_{21}^*(z, \omega) \\ & \times \mathbf{E}_{12}(z = 0, z = L, \Delta\omega)\exp(-i\Delta\mathbf{k}L) \\ & + \mathbf{H}_{21}(z, \omega)\mathbf{H}_{11}^*(z, \omega) \\ & \times [\mathbf{E}_{12}(z = 0, z = L, \Delta\omega) \\ & \times \exp(-i\Delta\mathbf{k}L)]^*, \end{aligned} \quad (18)$$

$$\begin{aligned}\mathbf{E}_{22}(z, \Delta\omega) = {} & \mathbf{H}_{12}(z, \omega)\mathbf{H}_{12}^*(z, \omega)\mathbf{E}_{11}(z = 0, \Delta\omega) \\ & + \mathbf{H}_{22}(z, \omega)\mathbf{H}_{22}^*(z, \omega)\mathbf{E}_{22}(z = L, \Delta\omega) \\ & + \mathbf{H}_{12}(z, \omega)\mathbf{H}_{22}^*(z, \omega) \\ & \times \mathbf{E}_{12}(z = 0, z = L, \Delta\omega)\exp(-i\Delta\mathbf{k}L) \\ & + \mathbf{H}_{22}(z, \omega)\mathbf{H}_{12}^*(z, \omega) \\ & \times [\mathbf{E}_{12}(z = 0, z = L, \Delta\omega) \\ & \times \exp(-i\Delta\mathbf{k}L)]^*, \end{aligned} \quad (19)$$

$$\begin{aligned}\mathbf{E}_{12}(z, z, \Delta\omega) = {} & \exp(i2\Delta\mathbf{k}z)\{\mathbf{H}_{11}(z, \omega)\mathbf{H}_{12}^*(z, \omega) \\ & \times \mathbf{E}_{11}(z = 0, \Delta\omega) \\ & + \mathbf{H}_{21}(z, \omega)\mathbf{H}_{22}^*(z, \omega) \\ & \times \mathbf{E}_{22}(z = L, \Delta\omega) \\ & + \mathbf{H}_{11}(z, \omega)\mathbf{H}_{22}^*(z, \omega) \\ & \times \mathbf{E}_{12}(z = 0, z = L, \Delta\omega) \\ & \times \exp(-i\Delta\mathbf{k}L) + \mathbf{H}_{21}(z, \omega)\mathbf{H}_{12}^*(z, \omega) \\ & \times [\mathbf{E}_{12}(z = 0, z = L, \Delta\omega) \\ & \times \exp(-i\Delta\mathbf{k}L)]^*\}. \end{aligned} \quad (20)$$

Note that the spectral-density functions $\mathbf{E}_{11}(z = 0, \Delta\omega)$, $\mathbf{E}_{22}(z = L, \Delta\omega)$, and $\mathbf{E}_{12}(z_1 = 0, z_2 = L, \Delta\omega)$ of the two inputs $\mathbf{E}_1(z = 0, t)$ and $\mathbf{E}_2(z = L, t)$ are given as the boundary conditions.

Two physical processes happen simultaneously during two-wave mixing in a photorefractive medium. First, the two optical waves propagate through the photorefractive medium while being scattered into each other by the index grating. Second, the scattered waves modify the index grating through the photorefractive effect until a steady state is reached. We have provided above a mathematical model that describes these two physical processes separately. A steady state of the two-wave mixing in the photorefractive medium is reached when the two optical waves scattered by the photorefractive grating can

exactly sustain the same photorefractive grating. A steady-state solution of the two-wave mixing in a photorefractive medium can thus be obtained by use of the mathematical model described above through an iterative procedure. The procedure is outlined as follows:

Step 1: Give an initial guess on the function $\mathbf{Q}(z)/I_0(z)$.

Step 2: Solve Eqs. (12) and (13) for the functions $\mathbf{H}_{ij}(z, \omega)$ $(i, j = 1, 2)$ with the function $\mathbf{Q}(z)/I_0(z)$ provided in the last step.

Step 3: Obtain the spectral-density functions $\mathbf{E}_{11}(z, \Delta\omega)$, $\mathbf{E}_{22}(z, \Delta\omega)$, and $\mathbf{E}_{12}(z, z, \Delta\omega)$ by use of Eqs. (18)–(20).

Step 4: Obtain $I_1(z)$, $I_2(z)$, $\mathbf{Q}(z)$, and $\mathbf{Q}(z)/I_0(z)$ by use of Eqs. (5), (6), (7), and (10).

Step 5: Compare the new version of the index grating $\mathbf{Q}(z)/I_0(z)$ and the previous version. If they are close within a certain accuracy requirement, the solution has been obtained. Otherwise, the iteration continues by use of the new version of the index grating.

To determine the boundary conditions, we assume that both the input optical waves are derived from the same laser source. If the source laser wave has a Gaussian line shape with a FWHM linewidth of $\delta\omega$, then the normalized spectral-density function of the source laser wave can be written as

$$\mathbf{E}_{ss}(\Delta\omega) = \frac{4(\pi \ln 2)^{1/2}}{\delta\omega} \exp\left\{-\left[2(\ln 2)^{1/2} \frac{\Delta\omega}{\delta\omega}\right]^2\right\}. \tag{21}$$

Taking β as the incident-intensity ratio $I_1(z = 0)/I_2(z = L)$ of the two optical waves at their respective entrance boundary planes, we obtain the boundary conditions as

$$\mathbf{E}_{11}(z = 0, \Delta\omega) = \beta \mathbf{E}_{ss}(\Delta\omega), \tag{22}$$

$$\mathbf{E}_{22}(z = 0, \Delta\omega) = \mathbf{E}_{ss}(\Delta\omega), \tag{23}$$

$$\mathbf{E}_{12}(z_1 = 0, z_2 = L, \Delta\omega) = \sqrt{\beta}\mathbf{E}_{ss}(\Delta\omega)\exp(-i\mathbf{k}_0 L) \times \exp(-i\omega t_d), \tag{24}$$

where t_d is the time delay between the optical waves when they reach their respective entrance planes. In deriving the above boundary conditions, we have assumed that the laser source has a Gaussian line shape. There is no loss of generality in this assumption. Similar results can be obtained with a different line shape.

This completes the general formulation to model contradirectional two-wave mixing in photorefractive crystals.

3. DISCUSSIONS AND SIMULATIONS

To clarify the complicated formulation described above, we consider some simple cases first before presenting the numerical and experimental results.

In the absence of coupling ($\gamma = 0$) in a lossless medium ($\alpha = 0$) with $\beta = 1$ the above formulation describes the interference of two counterpropagating optical waves in a dielectric medium. In this case it takes only one iteration to obtain the solution, which is

$$\mathbf{E}_{12}(z, z, \Delta\omega) = \mathbf{E}_{ss}(\Delta\omega)\exp(-i\mathbf{k}L) \times \exp(-i\omega t_d)\exp(2i\Delta\mathbf{k}z). \tag{25}$$

Fourier transforming the above equation over ω and taking into account the extra phase term $\exp(2i\mathbf{k}_0 z)$ resulted from the definition of $\mathbf{E}_1(z, t)$ and $\mathbf{E}_2(z, t)$ in Eq. (1), we obtain the mutual coherence of the two waves as a function of position z,

$$\Gamma_{12}(z, \tau) = \Gamma_s\left(\tau + t_d + \frac{nL - 2nz}{c}\right)\exp(-i\omega_0 t_d), \tag{26}$$

where $\Gamma_s(\tau)$ is the normalized self-coherence function of the source laser wave and n is the index of refraction of the medium. The result has been well established in the literature. This example can also help us see more clearly the subtle contribution of the phase terms in the above formulation. In our definition, $t_d = 0$ if $z = L/2$ is the plane of zero path difference.

When the coherence time $\delta\omega^{-1}$ is much larger than the time delay involved in the above formulation, i.e., $\delta\omega t_d \ll 1$ and $\delta\omega nL/c \ll 1$, the normalized spectral-density function of the source laser wave can be written as $\mathbf{E}_{ss}(\omega) = \delta(\omega - \omega_0)$. From the above formulation we can obtain the set of equations governing the intensities of the two optical waves,

$$\frac{\mathrm{d}}{\mathrm{d}z} I_1 = \gamma \frac{I_1 I_2}{I_1 + I_2} - \alpha I_1, \tag{27}$$

$$\frac{\mathrm{d}}{\mathrm{d}z} I_1 = \gamma \frac{I_1 I_2}{I_1 + I_2} + \alpha I_1. \tag{28}$$

These two equations are exactly the same as those obtained for two-wave mixing of monochromatic waves. We note that $\delta\omega t_d \ll 1$ is a condition for partially coherent waves to be treated as monochromatic waves in contradirectional two-wave mixing in a photorefractive medium. We also recall that the upper limit on the coherence time, i.e., $\delta\omega\tau_{ph} \gg 1$, still needs to be satisfied to reach Eqs. (27) and (28) from the above general formulation. This is the main difference between the results of Eqs. (27) and (28) in this paper and those obtained directly for monochromatic waves. Note that we did not use the iterative procedure in obtaining Eqs. (27) and (28). The complete boundary conditions for Eqs. (27) and (28) are simply $I_1(z = 0)$ and $I_2(z = L)$.

We now use the above general formulation to obtain the solution in the nondepleted-pump regime (for $\gamma \neq 0$), which has been obtained previously by a different method. Using Eqs. (12) and (13) and the following three definitions,

$$\mathbf{E}_{11}(z, \Delta\omega) = \langle \tilde{\mathbf{E}}_1(z, \omega)\tilde{\mathbf{E}}_1^*(z, \omega)\rangle, \tag{29}$$

$$\mathbf{E}_{22}(z, \Delta\omega) = \langle \tilde{\mathbf{E}}_2(z, \omega)\tilde{\mathbf{E}}_2^*(z, \omega)\rangle, \tag{30}$$

$$\mathbf{E}_{12}(z, z, \Delta\omega) = \langle \tilde{\mathbf{E}}_1(z, \omega)\tilde{\mathbf{E}}_2^*(z, \omega)\rangle\exp(2i\Delta\mathbf{k}z), \tag{31}$$

we can obtain a set of equations governing the propagation of the spectral-density functions as

$$\frac{\partial \mathbf{E}_{11}(z,\,\Delta\omega)}{\partial z} = \frac{\gamma}{2I_0(z)}\,[\mathbf{Q}(z)\mathbf{E}_{12}{}^{*}(z,\,z,\,\Delta\omega) + \mathbf{Q}^{*}(z)\mathbf{E}_{12}(z,\,z,\,\Delta\omega)] - \alpha\mathbf{E}_{11}(z,\,\Delta\omega), \tag{32}$$

$$\frac{\partial \mathbf{E}_{22}(z,\,\Delta\omega)}{\partial z} = \frac{\gamma}{2I_0(z)}\,[\mathbf{Q}(z)\mathbf{E}_{12}{}^{*}(z,\,z,\,\Delta\omega) + \mathbf{Q}^{*}(z)\mathbf{E}_{12}(z,\,z,\,\Delta\omega)] + \alpha\mathbf{E}_{22}(z,\,\Delta\omega), \tag{33}$$

$$\frac{\partial \mathbf{E}_{12}(z,\,z,\,\Delta\omega)}{\partial z} = 2i\Delta\mathbf{k}\mathbf{E}_{12}(z,\,z,\,\Delta\omega) + \frac{\gamma}{2I_0(z)}\,\mathbf{Q}(z) \times [\mathbf{E}_{11}(z,\,\Delta\omega) + \mathbf{E}_{22}(z,\,\Delta\omega)] - \alpha\mathbf{E}_{12}(z,\,z,\,\Delta\omega). \tag{34}$$

$\tilde{\mathbf{E}}_1(z,\,\omega)$ and $\tilde{\mathbf{E}}_2(z,\,\omega)$ in Eqs. (29)–(31) are related to the Fourier-transform coefficients of the two optical waves as defined in Eq. (11). Strictly speaking, a stationary random process cannot be Fourier transformed over the time variable t. However, we can truncate it into a finite duration T and Fourier transform the truncated process. After that, we can first obtain a set of equations similar to Eqs. (32)–(34) for the truncated process, then let T go to infinity to obtain Eqs. (32)–(34). This is a standard procedure in statistical optics.[10] Fourier transforming the above relation over $\Delta\omega$, we obtain a set of equations governing the propagation of the self and mutual coherence of the two optical waves as

$$\frac{\partial \Gamma_{12}(z,\,\tau)}{\partial z} = -\frac{2n}{c}\,\frac{\partial \Gamma_{12}(z,\,\tau)}{\partial \tau} + \frac{\gamma}{2}\,\frac{\Gamma_{12}(z,\,0)}{I_1 + I_2} \times [\Gamma_{11}(z,\,\tau) + \Gamma_{22}(z,\,\tau)], \tag{35}$$

$$\frac{\partial \Gamma_{11}(z,\,\tau)}{\partial z} = \frac{\gamma}{2}\,\frac{\Gamma_{12}(z,\,0)}{I_1 + I_2}\,\Gamma_{12}{}^{*}(z,\,-\tau) + \frac{\gamma}{2}\,\frac{\Gamma_{12}{}^{*}(z,\,0)}{I_1 + I_2}\,\Gamma_{12}(z,\,\tau) - \alpha\Gamma_{11}(z,\,\tau), \tag{36}$$

$$\frac{\partial \Gamma_{22}(z,\,\tau)}{\partial z} = \frac{\gamma}{2}\,\frac{\Gamma_{12}(z,\,0)}{I_1 + I_2}\,\Gamma_{12}{}^{*}(z,\,-\tau) + \frac{\gamma}{2}\,\frac{\Gamma_{12}{}^{*}(z,\,0)}{I_1 + I_2}\,\Gamma_{12}(z,\,\tau) + \alpha\Gamma_{22}(z,\,\tau). \tag{37}$$

When there is no absorption in the photorefractive medium (i.e., $\alpha = 0$), we can obtain, from Eqs. (36) and (37),

$$\frac{\partial}{\partial z}\,[\Gamma_{11}(z,\,\tau) - \Gamma_{22}(z,\,\tau)] = 0. \tag{38}$$

Further, letting $\tau = 0$ in Eq. (38), we obtain

$$\frac{\partial}{\partial z}\,[I_1(z) - I_2(z)] = 0. \tag{39}$$

Equation (39) shows that, when there is no absorption in the photorefractive medium, the intensity difference between the signal wave and the pump wave is a constant of integration (conservation of power flow).

Note that, although Eqs. (35)–(37) are general and self-consistent, they contain only the mutual coherence of the two optical waves at the same locations. They are not compatible with the kind of boundary conditions as given by Eq. (24), which gives the mutual statistical properties of the two waves at two different points in space. Therefore they are useful only in the nondepleted-pump regime, where we can assume that the pump wave passes through the photorefractive medium without changing its statistical properties. Under this assumption we can obtain from Eqs. (22)–(24) the self- and mutual-coherence functions of the two waves at the signal-wave entrance boundary plane ($z = 0$) as

$$\Gamma_{12}(z = 0,\,\tau) \equiv \sqrt{\beta}\,\Gamma_{ss}(\tau + \delta t)\exp(-i\omega_0\delta t), \tag{40}$$

$$\Gamma_{11}(z = 0,\,\tau) \equiv \beta\Gamma_{ss}(\tau), \tag{41}$$

$$\Gamma_{22}(z = 0,\,\tau) \equiv \Gamma_{ss}(\tau), \tag{42}$$

where $\delta t = t_d + nL/c$ is the time delay between the two optical waves at the signal-wave entrance plane and

$$\Gamma_{ss}(\tau) = \exp\left\{-\left[\frac{\delta\omega\tau}{4(\ln 2)^{1/2}}\right]^2\right\} \tag{43}$$

is the coherence function of the source laser wave. We can use Eqs. (40)–(42) as the boundary conditions and integrate Eqs. (35)–(37).

Equations (35)–(37) are simple not only in the sense that they can be implemented easily numerically, but also that they can be used to obtain approximate analytical solutions to some special cases within the nondepleted regime. One such case is that the coherence length of the source laser wave is much longer than the two-wave-mixing interaction length and the coupling constant is large. This occurs when we use a multimode argon laser and a $KNbO_3$:Co crystal for the two-wave-mixing experiment. In this case we can neglect the term that contains the partial derivative on τ in Eq. (35) and reduce the set of partial differential equations, i.e., Eqs. (35)–(37), to a set of ordinary differential equations that can be solved analytically under the nondepleted-pump approximation. Remember that Eq. (35) is derived directly from Eq. (34). We can see from Eq. (34) that the approximation of neglecting the term that contains the partial derivative on τ in Eq. (35) implies that the wave-vector difference $\Delta\mathbf{k}$ of the different frequency components of the two partially coherent waves are negligible with respect to the thickness of the photorefractive medium (i.e., $\Delta\mathbf{k}L \ll 1$). Similar approximation has been made previously by Saxena *et al.* in the study of multiple-beam interaction by transmission gratings in the photorefractive media.[12,13] Therefore under the nondepleted-pump approximation and the approximation of $\Delta\mathbf{k}L \ll 1$ the signal-wave intensity gain and the normalized mutual coherence of the two waves can be obtained as

$$\frac{I_1(z)}{I_1(0)} \equiv \frac{\Gamma_{11}(z,\,0)}{\Gamma_{11}(0,\,0)} = \frac{\Gamma_{12}(0,\,0)\Gamma_{12}{}^{*}(0,\,0)}{\Gamma_{11}(0,\,0)\Gamma_{22}(0,\,0)} \times [\exp(\gamma z) - 1]\exp(-\alpha z) + \exp(-\alpha z), \tag{44}$$

$$\gamma_{12}(z) \equiv \frac{\Gamma_{12}(z, 0)}{[\Gamma_{11}(z, 0)\Gamma_{22}(z, 0)]^{1/2}} = \frac{1}{\left\{\dfrac{\Gamma_{12}^{*}(0, 0)}{\Gamma_{12}(0, 0)}[1 - \exp(-\gamma z)] + \dfrac{\Gamma_{11}(0, 0)\Gamma_{22}(0, 0)}{\Gamma_{12}^{2}(0, 0)}\exp(-\gamma z)\right\}^{1/2}}. \quad (45)$$

In most photorefractive crystals with $\exp[(\gamma - \alpha)z] \gg 1$ the signal-intensity gain is affected primarily by $(\gamma - \alpha)$. We also note that the normalized mutual coherence of the two waves is affected only by the photorefractive coupling constant γ.

As a comparison of the general formulation, the simplified formulation and the approximate analytical solutions, we show in Figs. 2 and 3 the signal-intensity gain and the normalized mutual coherence of the two waves at the signal-wave exit plane $(z = L)$ as a function of the optical path difference between the two optical waves at the signal-wave entrance plane $(z = 0)$. The parameters are $\gamma = 3.0\ \mathrm{cm}^{-1}$, $\alpha = 0.0\ \mathrm{cm}^{-1}$, $n = 2.3$, $L = 0.72$ cm, and $\delta\omega = 2\pi \times 1.8$ GHz, and $\beta = 10^{-4}$. These are typical parameters in our experiment when we use a multimode argon laser and a $KNbO_3$:Co crystal to implement the two-wave-mixing experiment. In this case the coherence length of the source laser wave is much longer than the thickness of the photorefractive medium. The general formulation and the simplified formulation produce the same results within the numerical accuracy in the nondepleted regime. The results of these two formulations are represented by the dashed curves in Figs. 2 and 3. We notice that the approximate analytical solution retains the major characteristics of the exact solution and provides a good understanding of the interaction. The results of the approximate analytical solution are represented by the solid curves in the figures. Note that the curves obtained from the approximate analytical solution are symmetric about $z_0 = 0$ owing to the approximation of neglecting the partial derivative over τ in Eq. (35), while the curves obtained from the general formulation are shifted to the right side (see Figs. 2 and 3). Here, z_0 is defined as the path difference. The difference between the results of the approximate analytical solution and those of the general formulation will decrease as the ratio between the coherence length of two waves and the thickness of the photorefractive medium increases.

Now let us consider the case of the depleted pump. Numerical simulation with the general formulation is the only means to analyze this case. We first consider the case in which the coherence length of the source laser wave is finite but much longer than the thickness of the photorefractive medium. Again, we use the following set of parameters: $\gamma = 3.0\ \mathrm{cm}^{-1}$, $\alpha = 0.0\ \mathrm{cm}^{-1}$, $n = 2.3$, $L = 0.72$ cm, and $\delta\omega = 2\pi \times 1.8$ GHz. The solid curves in Fig. 4 show the signal intensity $I_1(z)$, the pump intensity $I_2(z)$, and the normalized mutual coherence $\gamma(z) = \Gamma_{12}(z, 0)/[\Gamma_{11}(z, 0)\Gamma_{22}(z, 0)]^{1/2}$ as functions of the position z in the photorefractive medium. The optical path difference between the signal wave and the pump wave at the signal-wave entrance boundary $(z = 0)$ is chosen to be zero. The incidence intensity ratio β of the two waves is chosen to be one. We also show in Fig. 4 with dashed curves the signal intensity $I_1(z)$ and the pump intensity $I_2(z)$ for two-wave mixing with monochromatic waves for the purpose of comparison. We notice that the results of two-wave mixing with partially coherent waves are very close to those of two-wave mixing with

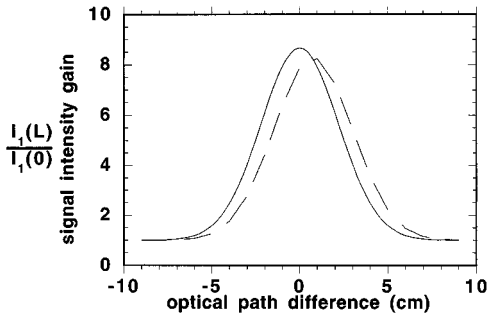

Fig. 2. Signal-wave intensity gain as a function of the optical-path difference at the signal-wave entrance plane in the nondepleted-pump regime. The dashed curve is the numerical solution. The solid curve is the approximate analytical solution.

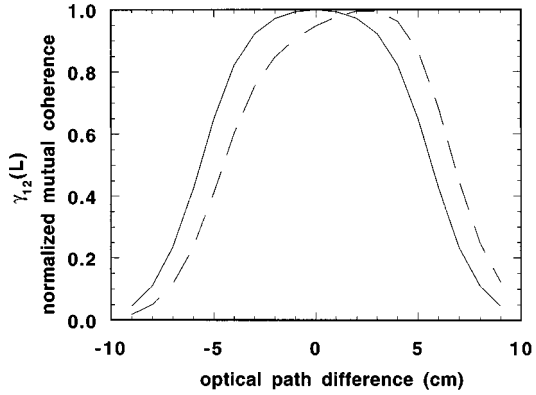

Fig. 3. Mutual coherence of the two waves at the signal-wave exit plane as a function of the optical path difference at the signal-wave entrance plane in the nondepleted-pump regime. The dashed curve is the numerical solution. The solid curve is the approximate analytical solution.

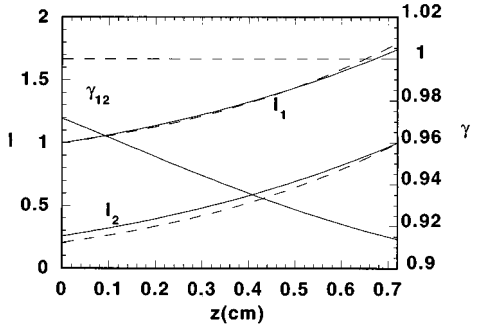

Fig. 4. Signal intensity, pump intensity, and the normalized mutual coherence as a function of position z in the photorefractive medium for partially coherent waves (solid curves) and monochromatic waves (dashed curves).

monochromatic waves when the optical path difference of the two waves is small compared with the coherence length of the source laser wave. The effect of partial coherence of the two waves in this case is significant only for a large optical path difference of the two waves. We show the signal-intensity gain in Fig. 5(a) and the mutual coherence between the signal wave and the pump wave at the pump-wave entrance plane ($z = L$) in Fig. 5(b) both as functions of the optical path difference between the two waves at the signal-wave entrance plane ($z = 0$) for various intensity ratios β. Figure 5(a) shows that the signal-intensity gain decreases as the optical path difference of the two waves increases until there is no coupling between the two waves when the optical path difference of the two waves exceeds the coherent length of the source laser wave. The same figure also shows that the signal-intensity gain increases as the intensity ratio β decreases until the signal-intensity gain saturates as the nondepleted-pump regime is reached. Figure 5(b) shows that the normalized mutual coherence of the two waves at the pump-wave entrance plane ($z = L$) decreases as the intensity ratio β of the two waves increases. When β is much larger than one, the signal wave will pass through the photorefractive medium with its statistical properties almost unchanged by coupling. In this limit the normalized mutual coherence of the two waves at the pump-wave entrance plane ($z = L$) with coupling will be the same as that for an arbitrary β but without coupling. We note that the normalized mutual coherence of the two waves at the pump-wave entrance plane ($z = L$) is enhanced by coupling. Figure 5(b) also shows that the normalized mutual coherence decreases quickly as the optical path difference gets close to and larger than the coherence length of the source laser wave.

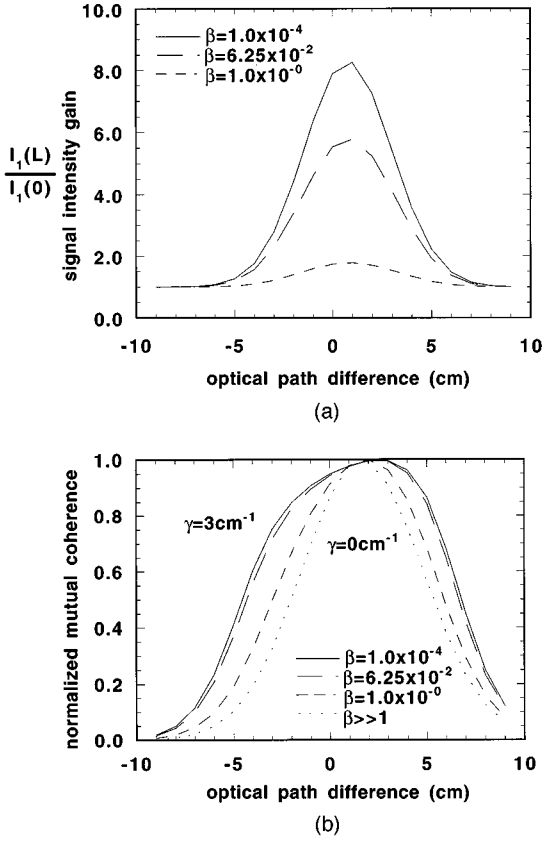

Fig. 5. (a) Signal-intensity gain and (b) the normalized mutual coherence of the two waves at the pump-wave entrance plane ($z = L$) as functions of the optical path difference at the signal-wave entrance plane ($z = 0$) for a coupling constant $\gamma = 3\ \mathrm{cm}^{-1}$ and various intensity ratios between the signal wave and the pump wave. Note that the curve for a coupling constant $\gamma = 3\ \mathrm{cm}^{-1}$ and $\beta \gg 1$ is the same as that for a coupling constant $\gamma = 0\ \mathrm{cm}^{-1}$ and an arbitrary β.

Second, we consider the case that the coherence length of the source laser wave is shorter than the thickness of the photorefractive medium. The following parameters are chosen in the simulation: $\alpha = 0.0\ \mathrm{cm}^{-1}$, $n = 2.3$, $L = 2.0$ cm, $\delta\omega = 2\pi \times 18$ GHz, and $t_d = -nL/c$. $t_d = -nL/c$ implies that the optical path difference between the signal wave and the pump wave is zero at the signal-wave entrance plane ($z = 0$). Since the spectral line shape of the source laser wave is assumed to be Gaussian, the coherence length of the source laser wave inside the photorefractive medium is $L_c = 2\pi \times 0.664c/(n\,\delta\omega) = 0.48$ cm. In Fig. 6 we show the signal intensity $I_1(z)$ and the grating profile $\mathbf{Q}(z)/I_0(z)$ as functions of the position z inside the photorefractive medium for an incident intensity ratio $\beta = 1$ and a coupling constant $\gamma = 20\ \mathrm{cm}^{-1}$. We note that the length of the photorefractive grating is limited by the partial coherence of the two interacting waves and that the pump depletion is moderate even for a very large coupling constant. In Figs. 7(a) and 7(b) we show the signal intensity $I_1(z)$ and the grating profile $\mathbf{Q}(z)/I_0(z)$ as functions of the position z inside the photorefractive medium for an incident intensity ratio $\beta = 10^{-4}$ and coupling constants $\gamma = 10\ \mathrm{cm}^{-1}$ and $\gamma = 20\ \mathrm{cm}^{-1}$, respectively. We note that the length of the photorefractive grating is increased but still primarily limited by the partial coherence of the two interacting waves for a small incident intensity ratio and a small coupling constant. Figure 7(b) shows that the length of the photorefractive grating is no longer limited by the partial coherence of the two interacting waves for a small incident intensity ratio and a large coupling constant. The length of the photorefractive grating in this case is limited by the length of the photorefractive medium, which is much longer than the coherence length of the interacting waves. The photorefractive grating is a temporally stationary index grating. When the incident intensity ratio is small, the amplified signal wave at its exit plane ($z = L$) is primarily the incident pump wave reflected by the photorefractive grating, and the depleted pump wave at its exit plane ($z = 0$) is primarily the incident pump wave transmitted through the photorefractive grating. When the length of the photorefractive grating is comparable to or longer than the coherence length of the source laser wave inside the photorefractive medium, the output waves $\mathbf{E}_1(L)$ and $\mathbf{E}_2(0)$ may have spectra different from those of the input waves $\mathbf{E}_1(0)$ and $\mathbf{E}_2(L)$ owing to the presence of the photorefractive grating, which acts as a spectral filter. In Figs. 8(a) and 8(b) we show the normalized spectra of the amplified signal wave and the depleted pump wave at their respective exit planes, using the same sets of parameters as those used to obtain Figs. 7(a) and 7(b), respectively. We note that the amplified signal wave has a bandwidth narrower than that of the

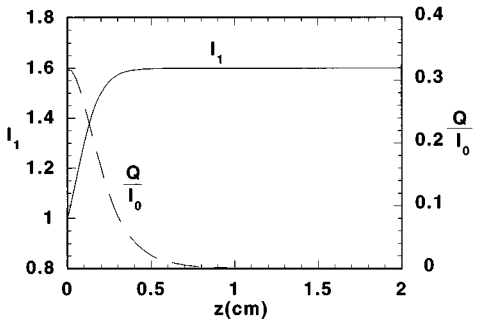

Fig. 6. Signal intensity $I_1(z)$ (solid curve) and the grating profile $\mathbf{Q}(z)/I_0(z)$ (dashed curve) as functions of the position z inside the photorefractive medium for an incident intensity ratio $\beta = 1$ and a coupling constant $\gamma = 20\ \mathrm{cm}^{-1}$.

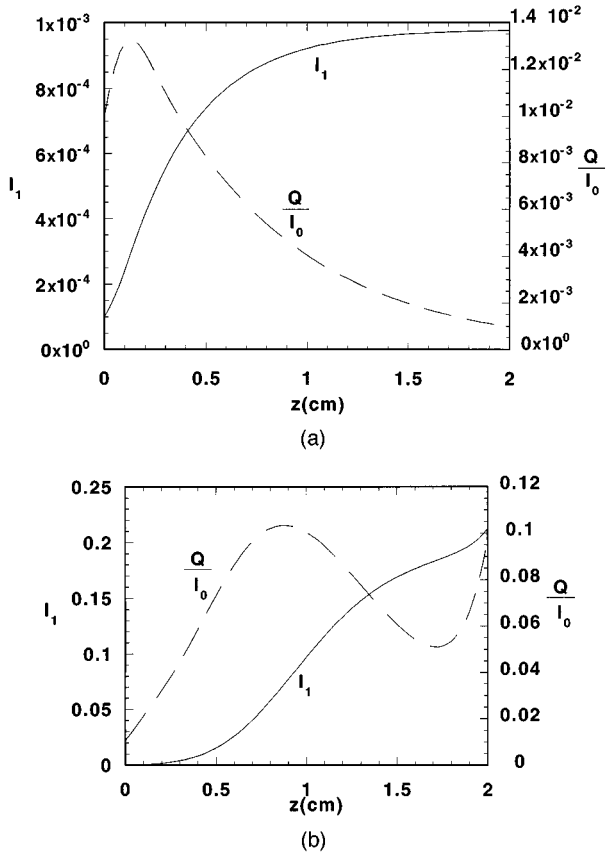

Fig. 7. Signal intensity $I_1(z)$ (solid curve) and the grating profile $\mathbf{Q}(z)/I_0(z)$ (dashed curve) as functions of the position z inside the photorefractive medium for an incident intensity ratio $\beta = 10^{-4}$ and coupling constants (a) $\gamma = 10\ \mathrm{cm}^{-1}$ and (b) $\gamma = 20\ \mathrm{cm}^{-1}$.

incident pump wave. Furthermore, the bandwidth of the amplified signal wave decreases as the length of the photorefractive grating increases. In Fig. 8(a), since the coupling constant is small, the pump-wave depletion is small ($\gamma = 10\ \mathrm{cm}^{-1}$) and the spectrum of the transmitted pump wave is almost the same as that of the incident pump wave. In Fig. 8(b), since the coupling constant is large ($\gamma = 20\ \mathrm{cm}^{-1}$), the pump depletion is significant. The central part of the incident pump-wave spectrum is depleted most significantly, and therefore the transmitted pump wave has a different spectrum from the incident pump wave. According to the spectra shown in Fig. 8, the case considered in Fig. 7(a) and Fig. 8(a) is in the nondepleted-pump regime, and the case considered in Fig. 7(b) and Fig. 8(b) is in the depleted-pump regime, although both cases seem to be in the nondepleted-pump regime when we look only at the signal intensity. In Figs. 9(a) and 9(b) we show with solid curves the normalized mutual coherence of the two waves as a function of position z, again using the same sets of parameters as those used to obtain Figs. 7(a) and 7(b), respectively. For comparison we show in these two figures with dashed curves the normalized mutual coherence of the two waves as a function of position z without coupling. In Fig. 9(a) the normalized mutual coherence of the two waves is the same with coupling as that without coupling in the region $z < 0$ and is increased in the region $z > L$ owing to coupling; in Fig. 9(b) the normalized mutual coherence of the two waves is decreased in the region close to plane $z = 0$. The increase of mutual coherence in both Figs. 9(a) and 9(b) can be attributed to the reflection of the strong pump wave in the direction of the weak signal wave by the stationary photorefractive index grating. The decrease of mutual coherence in Fig. 9(b) can be attributed to the spectral-filtering effect of the photorefractive index grating on the pump wave. There is no decrease of mutual coherence in the region close to plane $z = 0$ in Fig. 9(a) because pump depletion and therefore the spectral-filtering effect on the pump wave are negligible in this case.

Third, when a laser beam enters a photorefractive crystal, scattering occurs because of surface pits, imperfec-

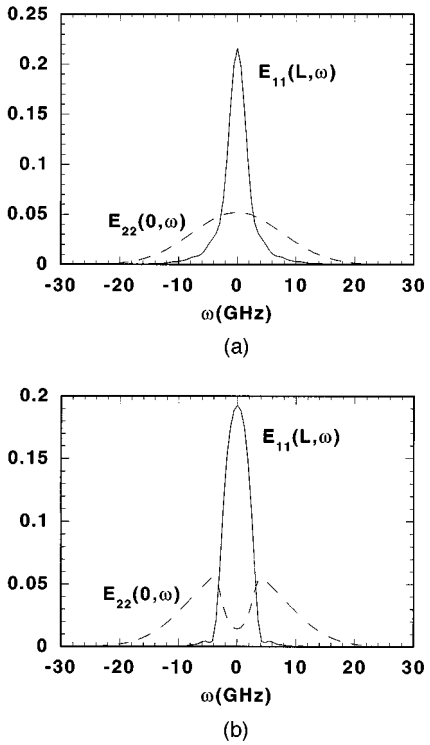

Fig. 8. Normalized spectra of the amplified signal wave (solid curve) and the depleted pump wave (dashed curve) at their respective exit planes for an incident intensity ratio $\beta = 10^{-4}$ and coupling constants (a) $\gamma = 10\ \mathrm{cm}^{-1}$ and (b) $\gamma = 20\ \mathrm{cm}^{-1}$.

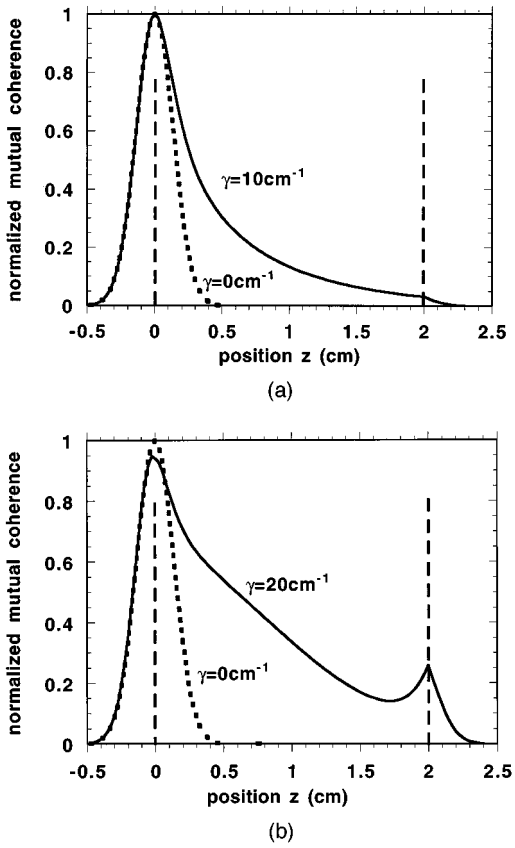

Fig. 9. Normalized mutual coherence of the two waves as functions of position z for an incident intensity ratio $\beta = 10^{-4}$ and for coupling constants (a) $\gamma = 10\ \mathrm{cm}^{-1}$ (solid curve) and $\gamma = 0\ \mathrm{cm}^{-1}$ (dashed curve) and (b) $\gamma = 20\ \mathrm{cm}^{-1}$ (solid curve) and $\gamma = 0\ \mathrm{cm}^{-1}$ (dashed curve).

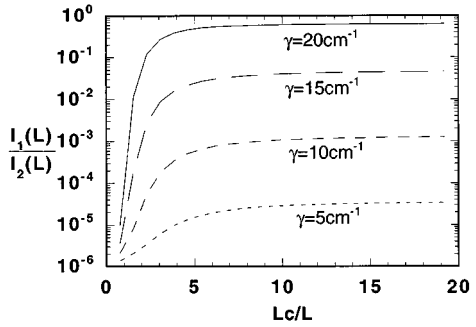

Fig. 10. Phase-conjugation reflectivity as a function of the coherence length of the incident beam for various value of the coupling constant γ.

tion, and defects in the crystal. The scattered light overlaps with the incident beam and they undergo two-wave mixing. Under the appropriate condition the scattered light can be amplified, leading to phenomena such as fanning and stimulated backscattering. In a manner very similar to stimulated Brillouin scattering the stimulated backward scattering in photorefractive media is a possible mechanism for self-pumped phase conjugation.[14,15] The general formulation developed in this paper can be employed to investigate the effect of coherence on self-pumped phase conjugation by $2\mathbf{k}$ gratings. We show in Fig. 10 the phase-conjugation reflectivity as a function of the coherence length of the incident beams for various value of the coupling constant γ. The parameters in this simulation are $n = 2.3$, $L = 0.72$ cm, $\alpha = 0.0\ \mathrm{cm}^{-1}$, and $\beta = 1.0 \times 10^{-6}$. The time delay of the two waves is assumed to be zero at the signal-wave entrance plane ($z = 0$). The coherence length of the incident beams is related to the bandwidth as $L_c = 2\pi \times 0.664c/\delta\omega$. We note that the phase-conjugation reflectivity increases as the coherence length of the incident beam increases and reaches to a constant when the coherence length of the incident beam is much longer than the thickness of the photorefractive medium. We also note that the phase-conjugation reflectivity increases as the coupling constant increases.

4. EXPERIMENTS

The above theory is validated experimentally. The experimental setup is shown in Fig. 11. We utilized a 45°-cut $KNbO_3$:Co crystal (the c axis is in the horizontal plane leaning toward the $z = 0$ face of the crystal, and the b axis is in the vertical direction). The measured parameters of the crystal are $\gamma = 3.3\ \mathrm{cm}^{-1}$, $\alpha = 0.5\ \mathrm{cm}^{-1}$, $n = 2.3$, and $L = 0.72$ cm. A multimode argon laser operating at 514 nm is used as the laser source with a measured FWHM bandwidth of 1.83 GHz. The extraordinary polarization of the laser wave is used in the experiment. As illustrated in Fig. 11, the signal wave and the pump wave, obtained by splitting the argon laser wave, propagate contradirectionally into the $KNbO_3$:Co crystal. The incident intensity ratio of the two waves is $\beta = 0.00151$. The power of the pump wave is maintained at ~50 mW. The optical path difference of the two waves at the signal-wave incident plane $z = 0$ is denoted as $\Delta L = L_2 - L_1$. To monitor the mutual coherence between the signal wave and the pump wave at the output plane $z = L$, we employed another reference wave ($\mathbf{E}_{2\mathrm{ref}}$) that was split from the pump wave $\mathbf{E}_2$. The optical path difference of $\mathbf{E}_1$ and $\mathbf{E}_{2\mathrm{ref}}$ waves was adjusted to be the same as that of $\mathbf{E}_1$ and $\mathbf{E}_2$ waves at the output plane $z = L$. By a simple homodyne technique, the in-

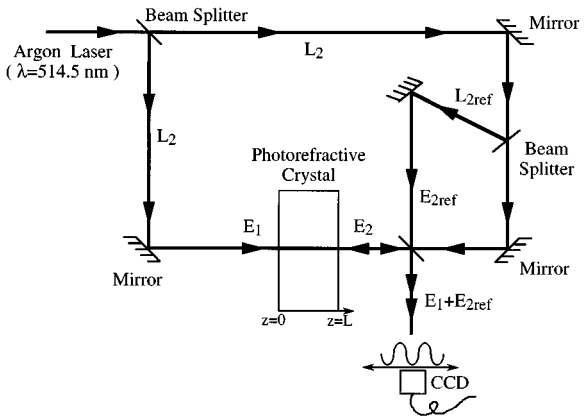

Fig. 11. Experimental setup. The distances L_1 and L_2 are the optical path length of the signal wave and the pump wave from laser source to the signal-wave incident plane $z = 0$, respectively. $L_{2\mathrm{ref}}$ is the optical path length of reference wave $E_{2\mathrm{ref}}$ from the laser source to the signal output plane $z = L$.

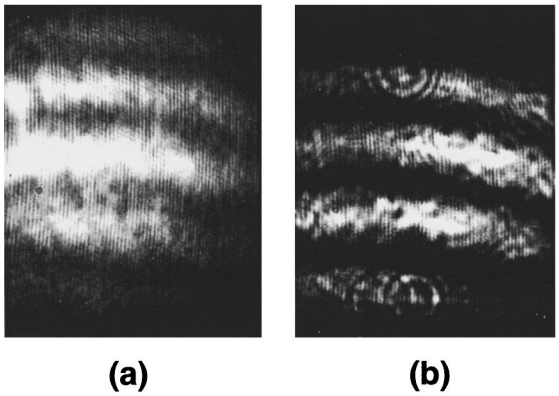

Fig. 12. Interference pattern of the signal wave and the reference wave at the output plane P1 (a) without photorefractive coupling and (b) with photorefractive coupling. Note the increase of fringe visibility that is due to the coupling.

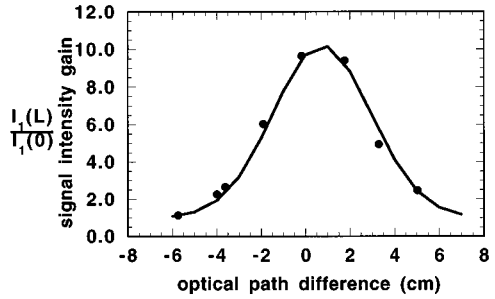

Fig. 13. Signal-intensity gain as a function of the optical path difference of the two waves at the signal-wave entrance plane ($z = 0$). The dots are experimental data, and the solid curve is the theoretical data.

terference fringes generated by $\mathbf{E}_1$ and $\mathbf{E}_{2\text{ref}}$ waves were observed by a CCD camera at the output plane $P1$. The normalized mutual coherence $\gamma_{12}(L)$ can be estimated as $(I_{\max} - I_{\min})/[4(I_1 I_2)^{1/2}]$, where $(I_{\max} - I_{\min})$ is the amplitude of the fringes. In our experiment we monitored the interference pattern with and without pump beam $\mathbf{E}_2$. Figure 12 shows the interference patterns with a normalized mutual coherence $\Gamma_{12}(0, 0) \approx 0.43$ at $z = 0$ ($\Delta L = 4$ cm). The measured normalized mutual coherence increases from 0.19 to 0.7 at $z = L$. The intensity gain of the signal wave was also measured. Figure 13 shows the measurement of the intensity gain (dots) of the signal wave at the $z = L$ plane as a function of the optical path difference ΔL. Along with the data is the theoretical curve for the same parameters. An excellent agreement between theory and experiment was achieved.

5. CONCLUSIONS

In conclusion, we have investigated theoretically contradirectional two-wave mixing with partially coherent waves in photorefractive crystals. A general formulation based on the theory of statistical properties of linear systems is provided.[16] Previous results on several simplified cases are rederived as special cases of the general formulation so that we can get more insight into the general formulation as well as into the simplified cases. Results of numerical implementation of the general formulation are also provided for various coupling constants and various incident intensity ratios between the signal wave and the pump wave. We found that the mutual coherence between the signal wave and the pump wave can be both increased and decreased owing to coupling. We also found that both the strength and the length of the photorefractive-index grating increases as the coupling constant increases. A photorefractive index grating much longer than the coherence length of the incident waves can be formed when the coupling constant is large and the incident intensity ratio is small. Owing to the spectral-filtering effect of the photorefractive-index grating, the spectra of the two interacting waves will be altered as they pass through the photorefractive medium. The general formulation is further used to model the effect of partial coherence on self-pumped phase conjugation by a $2\mathbf{k}$ grating. The theoretical predictions are in excellent agreement with experimental measurements.

APPENDIX A: ERGODICITY PROPERTY

In this appendix we provide the derivation of Eq. (10). Equation (9) gives the dynamics of the photorefractive index grating. It can be rewritten into an integration form as

$$\mathbf{Q}(z, t) = \frac{1}{\tau_{\text{ph}}} \int_{-\infty}^{t} \mathbf{E}_1(z, t')\mathbf{E}_2^*(z, t')\exp\left(\frac{t' - t}{\tau_{\text{ph}}}\right)\mathrm{d}t'. \tag{A1}$$

Note that $1/\tau_{\text{ph}}\int_{-\infty}^{t} \exp[(t' - t)/\tau_{\text{ph}}]\mathrm{d}t' = 1$. According to Eq. (A1), the grating amplitude $\mathbf{Q}(z, t)$ is approximately the average value of $\mathbf{E}_1(z, t')\mathbf{E}_2^*(z, t')$ over a time period τ_{ph}.

Since the optical wave amplitudes $\mathbf{E}_1(z, t)$ and $\mathbf{E}_2(z, t)$ are stationary random processes, the ensemble average $\langle \mathbf{E}_1(z, t)\mathbf{E}_2^*(z, t)\rangle$ is independent of the time variable t. Taking the ensemble average of Eq. (A1), we can obtain

$$\langle \mathbf{Q}(z, t)\rangle = \langle \mathbf{E}_1(z, t)\mathbf{E}_2^*(z, t)\rangle \equiv \Gamma_{12}(z, 0). \tag{A2}$$

Equation (A2) shows that the ensemble average of the grating amplitude $\mathbf{Q}(z, t)$ is equal to the mutual coherence of the two waves.

In general, the grating amplitude $\mathbf{Q}(z, t)$ is also a random variable. It fluctuates around its ensemble average. The mean square value of this random fluctuation, also called the variance of the random variable $\mathbf{Q}(z, t)$, can be written as

$$\langle |\mathbf{Q}(z, t) - \langle \mathbf{Q}(z, t)\rangle|^2\rangle = \langle |\mathbf{Q}(z, t)|^2\rangle - |\langle \mathbf{Q}(z, t)\rangle|^2. \tag{A3}$$

By using Eq. (A1), we can write the first term on the right side of Eq. (A3) explicitly as

$$\langle |\mathbf{Q}(z, t)|^2\rangle = \frac{1}{\tau_{\text{ph}}^2} \int_{-\infty}^{t}\int_{-\infty}^{t} \langle \mathbf{F}(z, t')\mathbf{F}^*(z, t'')\rangle \times \exp\left(\frac{t' - t}{\tau_{\text{ph}}}\right)\exp\left(\frac{t'' - t}{\tau_{\text{ph}}}\right)\mathrm{d}t'\mathrm{d}t'', \tag{A4}$$

where $\mathbf{F}(z, t) \equiv \mathbf{E}_1(z, t)\mathbf{E}_2^*(z, t)$ is a shorthand notation. Since the optical wave amplitudes $\mathbf{E}_1(z, t)$ and $\mathbf{E}_2(z, t)$ are stationary random processes, $\mathbf{F}(z, t)$ is also a stationary random process. Therefore the ensemble average $\langle \mathbf{F}(z, t')\mathbf{F}^*(z, t'')\rangle$ is a function of only two variables z and $t' - t''$. We define $\mathbf{R}(z, t' - t'') \equiv \langle \mathbf{F}(z, t')\mathbf{F}^*(z, t'')\rangle$ as a shorthand notation. With this relation we can change the integration arguments in Eq. (A4) from t' and t'' to $t_1 = t' + t'' - 2t$ and $t_2 = t' - t''$ and rewrite Eq. (A4) as

$$\langle |\mathbf{Q}(z, t)|^2\rangle = \frac{1}{2\tau_{\mathrm{ph}}^2} \int_{-\infty}^{0} \mathrm{d}t_1 \exp\left(\frac{t_1}{\tau_{\mathrm{ph}}}\right) \int_{t_1}^{-t_1} \mathrm{d}t_2 \mathbf{R}(z, t_2). \tag{A5}$$

Note that $1/(2\tau_{\mathrm{ph}}^2)\int_{-\infty}^{0}\mathrm{d}t_1 \exp(t_1/\tau_{\mathrm{ph}})\int_{t_1}^{-t_1}\mathrm{d}t_2 = 1$. Substituting Eqs. (A2) and (A5) into Eq. (A3), we can rewrite the variance of the grating amplitude $\mathbf{Q}(z, t)$ as

$$\begin{aligned}\langle |\mathbf{Q}(z, t) - \langle \mathbf{Q}(z, t)\rangle|^2\rangle &= \frac{1}{2\tau_{\mathrm{ph}}^2} \int_{-\infty}^{0} \mathrm{d}t_1 \exp\left(\frac{t_1}{\tau_{\mathrm{ph}}}\right) \int_{t_1}^{-t_1} \mathrm{d}t_2 [\mathbf{R}(z, t_2) \\ &\quad - |\Gamma_{12}(z, 0)|^2]. \end{aligned} \tag{A6}$$

Remember that $\mathbf{F}(z, t)$ is a stationary random process. Let Δt be the minimum time delay that is necessary for $\mathbf{F}(z, t)$ and $\mathbf{F}(z, t \pm \Delta t)$ to be uncorrelated. For $|t_2| \geqslant \Delta t$, $\mathbf{R}(z, t_2) - |\Gamma_{12}(z, 0)|^2$ is equal to zero. For $|t_2| \leqslant \Delta t$, $\mathbf{R}(z, t_2) - |\Gamma_{12}(z, 0)|^2$ is a function of t_2. Since both $\mathbf{R}(z, t_2)$ and $|\Gamma_{12}(z, 0)|^2$ are of the order of $I_1(z)I_2(z)$, the upper bound of $\mathbf{R}(z, t_2) - |\Gamma_{12}(z, 0)|^2$ can be written as $mI_1(z)I_2(z)$, where m is a constant factor of the order of unity. With these estimations we can obtain from Eq. (A6)

$$\langle |\mathbf{Q}(z, t) - \langle \mathbf{Q}(z, t)\rangle|^2\rangle < mI_1(z)I_2(z) \frac{\Delta t}{\tau_{\mathrm{ph}}}. \tag{A7}$$

According to relation (A7), the fluctuation of the grating amplitude $\mathbf{Q}(z, t)$ decreases as the ratio $\Delta t/\tau_{\mathrm{ph}}$ decreases. When $\Delta t/\tau_{\mathrm{ph}} \ll 1$, we can neglect the fluctuation of the grating amplitude $\mathbf{Q}(z, t)$ and obtain Eq. (10), i.e.,

$$\mathbf{Q}(z, t) \approx \langle \mathbf{Q}(z, t)\rangle = \Gamma_{12}(z, 0). \tag{A8}$$

Usually Δt is of the order of the coherence time $(\delta\omega)^{-1}$ of the incident waves. In this case the condition for Eq. (A8) can also be written as $\delta\omega\tau_{\mathrm{ph}} \gg 1$.

In this appendix we have shown that the time average of the random variable $\mathbf{E}_1(z, t)\mathbf{E}_2^*(z, t)$ is equal to the ensemble average of the random variable $\mathbf{E}_1(z, t)\mathbf{E}_2^*(z, t)$. This type of property is referred to as ergodicity in statistics.

ACKNOWLEDGMENTS

This research was supported by the U.S. Office of Naval Research and the U.S. Air Force Office of Scientific Research.

REFERENCES

1. See, for example, P. Yeh, *Introduction to Photorefractive Nonlinear Optics* (Wiley, New York, 1993).
2. See, for example, P. Gunter and J.-P. Huignard, eds., *Photorefractive Materials and Devices I and II*, Vols. 61 and 62 of Topics in Applied Physics (Springer-Verlag, Berlin, 1988, 1989).
3. B. Fischer, S. Sternklar, and S. Weiss, "Photorefractive oscillators," IEEE J. Quantum Electron. **25**, 550 (1989).
4. V. Wang, "Nonlinear optical phase conjugation for laser systems," Opt. Eng. **17**, 267 (1978).
5. S. C. De La Cruz, S. MacCormack, J. Feinberg, Q. B. He, H. K. Liu, and P. Yeh, "Effect of beam coherence on mutually pump phase conjugators," J. Opt. Soc. Am. B **12**, 1363 (1995).
6. Q. B. He and P. Yeh, "Photorefractive mutually pumped phase conjugation with partially coherent beams," Appl. Phys. B **60**, 47 (1995).
7. R. Hofmeister, A. Yariv, and S. Yagi, "Spectral response of fixed photorefractive grating interference filters," J. Opt. Soc. Am. A **11**, 1342 (1994).
8. N. V. Bogodaev, L. I. Ivleva, A. S. Korshunov, N. M. Polozkov, and V. V. Shkunov, "Increase of light-beam coherence by two-wave mixing in photorefractive crystals," J. Opt. Soc. Am. B **10**, 2287 (1993).
9. X. Yi, S. H. Lin, P. Yeh, and K. Y. Hsu, "Contradirectional two-wave mixing with partially coherent waves in photorefractive crystals," Opt. Lett. **21**, 1123 (1996).
10. See, for example, J. W. Goodman, *Statistical Optics* (Wiley, New York, 1985), Chap. 3.
11. P. Yeh, "Fundamental limit of the speed of photorefractive effect and its impact on device applications and material research," Appl. Opt. **26**, 602 (1987).
12. R. Saxena, F. Vachss, I. McMichael, and P. Yeh, "Diffraction properties of multiple-beam photorefractive gratings," J. Opt. Soc. Am. B **7**, 1210 (1990).
13. R. Saxena, C. Gu, and P. Yeh, "Properties of photorefractive gratings with complex coupling constants," J. Opt. Soc. Am. B **8**, 1047 (1991).
14. T. Y. Chang and R. W. Hellwarth, "Optical phase conjugation by backscattering in barium titanate," Opt. Lett. **10**, 108 (1985).
15. B. Ya. Zel'dovich, V. I. Popovichev, V. V. Ragul'skii, and F. S. Faizullov, "Connection between the wavefronts of the reflected and exciting light in SBS," Zh. Éksp. Teor. Fiz. **15**, 160 (1972).
16. A. W. Snyder, D. J. Mitchell, and Y. S. Kivshar, "Unification of linear and nonlinear wave optics," Mod. Phys. Lett. B **9**, 1479 (1995).